The Onset of the Last Interglacial and Fingerprints of Transient Atlantic Meridional Overturning Circulation

Paul Gierz (paul.gierz@awi.de)
Alfred Wegener Institute https://orcid.org/0000-0002-4512-087X

Gregor Knorr
Alfred Wegener Institute

Aline Govin
LSCE/IPSL https://orcid.org/0000-0001-8512-5571

Emilie Capron
Physics of Ice, Climate and Earth, Niels Bohr Institute, University of Copenhagen
https://orcid.org/0000-0003-0784-1884

Nadezhda Sokolova
Alfred Wegener Institute

Martin Werner
Alfred Wegener Institute https://orcid.org/0000-0002-6473-0243

Gerrit Lohmann
Alfred Wegener Institute https://orcid.org/0000-0003-2089-733X

Article

Keywords: glacials, interglacials, Atlantic Meridional Overturning Circulation

Posted Date: January 7th, 2021

DOI: https://doi.org/10.21203/rs.3.rs-131733/v1

Abstract

Transitions from glacials to interglacials are the largest climate shifts that occurred during the Quaternary. These glacial terminations are characterized by transient changes in the Atlantic Meridional Overturning Circulation (AMOC) and associated alterations in the northward heat transport. It has been a challenge to differentiate between early last interglacial or late penultimate glacial climate conditions at 129-131 ka (thousands of years before present). Neither simulations with a stable interglacial-type nor with a freshwater perturbed AMOC state have reproduced the reconstructed sea surface temperature (SST) fingerprint in the North Atlantic. As previous approaches failed to consider the highly transient nature of the climate system at ~130 ka, the potential of transient, deglaciating AMOC responses and the corresponding impact on North Atlantic SST has yet to be examined. In this study, we employ a fully coupled Atmosphere-Ocean General Circulation Model (AOGCM) equipped with a stable-oxygen isotope module to investigate the underlying AMOC dynamics at the onset of the Last Interglacial (LIG). We demonstrate that successfully capturing both the SST patterns and the calcite δ18O signature in planktonic foraminifera from North Atlantic marine sediment cores necessitates a transiently recovering AMOC. Furthermore, this critically depends on capturing the cold, glacial ocean state prior to the onset of the interglacial.

The Last Interglacial

Quaternary Interglacials are periods of Earth's history during which continental ice sheet volume and distribution were relatively similar to the Pre-Industrial (PI). They provide excellent testing grounds for our understanding of the Earth system's responses to orbital and greenhouse gas forcing[1]. The Last Interglacial (LIG) is the most recent interglacial prior to the Holocene. At this time, high-latitude surface ocean temperatures were warmer by at least 1˚C, and polar surface air temperatures by >3˚C relative to pre-industrial temperatures[2], and the global mean sea level was likely higher than present day by 6-9 meters[3,4]. Strong seasonal shifts in solar insolation changes as well as the preceding deglaciation played a major role in determining the high-latitude climate[2,3]. Attaining a full understanding of the LIG climate has been hampered by a series of challenges both from the perspective of paleoclimate simulations and from proxy-based reconstructions[1]. Modelling the LIG's climate has been thwarted by uncertainties in the configuration of continental ice sheets[5–7], the absolute timing of the prevailing atmospheric GHG concentrations[8], and, ultimately, the corresponding AMOC state and associated oceanic heat transport[9]. Several proxy-based ocean surface temperature syntheses are available for model-data comparison exercises across the LIG, but until recently they have had strong limitations. In particular, these syntheses did not realistically represent any specific time interval during the LIG, since they consisted either of one single snapshot[10,11] centered on the peak temperature or represented averaged conditions across the entire LIG interval[12]. In addition, they were based on paleorecords kept on their original timescales causing large dating uncertainties attached to the temperature estimates. Age discrepancies of up to 6 ka can be observed between records from various archives taken from different locations when the age scales are not harmonized[8]. However, the latest temperature syntheses are now based on a coherent temporal framework between paleorecords, and provide quantitative error estimates[12,13]. These syntheses provide a spatio-temporal description of the climate throughout the LIG and consist of multiple time slices of sea surface temperature anomalies relative to recent reference periods (from the recent Industrial Period or PI). Here, we focus on the time slice 129-131 ka (hereafter 130 ka). Data-based reconstructions indicate that the North Atlantic mean summer sea surface temperature (SSTs) at this time was 4.2 ± 0.8˚C cooler than PI[12]. To try and explain these cold SSTs, various studies have explored a potential mechanism involving remnant meltwater injection into the North Atlantic originating from Northern Hemisphere ice sheet melting throughout the penultimate deglaciation[14,15], which has been explored with several modelling studies[14,16]. Such meltwater events typically manifest as an asynchronous hemispheric pattern of temperature anomalies, with cooling in the North Atlantic accompanied by warming in the Southern Ocean (SO); proxy record syntheses indicate warming in the SO of 1.8±0.9˚C at the onset of the LIG. These types of signals are often recorded in proxy records during the transition from glacials to interglacials. A prominent example relevant for the onset of the LIG is Heinrich Event 11 (HE-11) showing exactly such a seesaw pattern[1,9,17,18]. An alternative scenario to explain the colder temperatures in the North Atlantic may be a transition out of the cold, glacial ocean state that prevailed during Termination II.

Considering the transient nature of the Earth System, climate and ice sheet changes during the LIG were influenced by the changes occurring throughout the penultimate deglaciation. In this context, adequately capturing the conditions at 130 ka with paleoclimate models is essential to better constrain the starting state for investigations of the LIG's transient evolution. Furthermore, clarifying the state of the ocean circulation at 130 ka is also critical to establish a clear definition of "full interglacial conditions". Such a definition would enable intercomparison between the different time periods, and ultimately allow us to deduce commonalities, differences, and the underlying mechanisms during the various Quaternary interglacials. Newer studies highlighted the difficulty in establishing a precise definition of an interglacial[17], and as such, it is difficult to determine if these cooler conditions in the North Atlantic region occur during the deglacial or interglacial interval. When defining the length of an interglacial using a threshold value on the ice dD isotope profile from the EPICA Dome C ice core[19], the 130 ka interval falls into the interglacial. However, the time period could also be categorized as part of the deglaciation interval when a definition based on global sea level is applied[20]. Thus, climate changes are apparently not occurring synchronously at 130 ka, thereby favoring a transient interpretation. Such a possibility has not yet been explored by climate simulations - previous modelling studies have examined the LIG from the perspective of a quasi-equilibrated climate state, either with[14] or without[21] freshwater influence. A conclusive understanding of the dynamics at work during this time could not be reached by these studies.

Possible Causes For A Cooler North Atlantic During The Early Last Interglacial

We hypothesize that the cooler North Atlantic temperatures are caused by a glacial/interglacial transition leading into the LIG rather than a fingerprint of a quasi-equilibrated AMOC weakening induced by freshwater forcing. To test our hypothesis, we use a temporally aligned synthesis of North Atlantic SSTs together with new reconstructions of the isotopic composition of seawater ($\delta^{18}O_{sw}$) and planktic foraminiferal calcite ($\delta^{18}O_c$) (Figure 1, see Methods and Supplementary Material for further details). Importantly, the temperature reconstructions are not based on oxygen isotopes, which allows us to separate temperature anomalies from oxygen isotope anomalies. The dataset shows distinct cooling of -3.4˚C ± 1.6˚C for summer SSTs in the North Atlantic (calculated as the July, August, and September average of 130ka minus core-top SST anomalies where the core-top is assumed to be a temporal average of the late Holocene, 3-0ka.) The uncertainty represents spatially averaged 1σ standard error based upon 17 locations. The same records show anomalies of +0.4‰ ± 0.3‰ $\delta^{18}O_c$ vs. PDB in planktic foraminifera, and -0.5‰ ± 0.6‰ $\delta^{18}O_{sw}$ vs. SMOW. The calculation of $\delta^{18}O_{sw}$ is based upon temperature and calcite reconstructions (for further details, see the Supplementary Material). We compare these reconstructions against fully coupled, stable oxygen isotope enabled ECHAM5/MPIOM-wiso simulations[21] forced by changes in atmospheric GHG concentrations[22–24] and orbital values[25] at 130 ka. We additionally perform a series of experiments including freshwater perturbations with varying injection rates (0.20 Sv, 0.10 Sv, and 0.05 Sv) and an isotopic signature of -30‰ $\delta^{18}O_{sw}$ (See Methods). We furthermore test the sensitivity of our model with respect to the injection location, performing an 0.20 Sv injection in the Ruddimann belt (henceforth IRD belt) in the North Atlantic, and alternatively in the Labrador and Nordic Seas. Finally, we examine a transient scenario, where the climate simulations are initialized from a glacial ocean state which mimics the deglacial history during Termination II (T-II). In order to maintain comparability with 130 ka anomalies vs. core-top values, we also perform a transient simulation of the Holocene from 3-0 ka, which is used as a control state (further details in the Supplementary Material).

Sensitivity To Freshwater Perturbation

The North Atlantic cooling reconstructed at 130 ka is typically interpreted as a fingerprint of a relatively weak AMOC circulation in response to meltwater input[13,14]. Deglacial meltwater stratified the upper North Atlantic, inhibiting deep-water formation, reducing northward oceanic heat transport, thus decreasing North Atlantic surface temperatures[26]. Including a freshwater perturbation in our model reproduces this behavior. Increasing the freshwater perturbation results in i) a more pronounced North Atlantic cooling relative to the unperturbed state (Figure 2a-d, left panel), and ii) a tendency towards more depleted values in both $\delta^{18}O_{sw}$ and $\delta^{18}O_c$. (Figure 2a-d, middle and right panels). Injecting freshwater into the North Atlantic IRD belt (Figure 2b-d) also leads to a weakening of North Atlantic Deep Water (NADW) formation, which increases with the magnitude of freshwater input (as demonstrated by the AMOC index, Figure 4a). Density anomalies are indeed transported from the central Atlantic to deep-water formation sites, which occurs in the Labrador and Nordic Seas in our model. Changing the location of freshwater injection from the IRD belt to the Labrador and Nordic Seas results in more pronounced North Atlantic cooling and

$\delta^{18}O_{sw}$ and $\delta^{18}O_c$ depletions (Figure 2e), because meltwater input now directly occurs over convection sites.

When compared to the reconstructions, the simulation without any freshwater influence yields ocean temperature anomalies which are too warm (LIG-PI Anomaly of -1.76, RMSE of 2.3 relative to the reconstructions), whereas including freshwater tends to over-estimate the cooling anomaly (LIG-PI anomaly (RMSE relative to reconstruction) of -3.56 (1.76), -4.03 (2.09), -4.17 (2.25) for the 0.05 Sv, 0.1 Sv, and 0.2 Sv injections). Changing the injection location leads to a further over-estimation of the anomaly (PI anomaly of -3.39, RMSE 2.19). For the isotopic signatures in seawater, increasing the injection strength leads to too depleted values (RMSE of 0.5, 0.8, and 1.14 for 0.05, 0.1, and 0.2 Sv); the simulation with an alternative injection again yields values which are too depleted (RMSE of 2.64). From this set of freshwater perturbation experiments, the 0.05 Sv injection into the IRD belt is best suited to reproduce the proxy reconstructions, yielding comparable temperature and isotopic anomalies.

We are able to disentangle and quantify three mechanisms influencing the $\delta^{18}O_c$ signature in foraminiferal calcite resulting from a freshwater perturbation (described in detail in the Supplementary Information) using our stable-oxygen isotope enabled simulation. This is achieved by re-performing the 0.2Sv injection experiment, but without modifying the isotopic signature of the seawater. This allows us to separate changes induced by the physical effects of a freshwater perturbation from the changes caused by injection meltwater with a strongly depleted $\delta^{18}O$ signature. With this technique, we are able to determine $\delta^{18}O_c$ changes purely due to oceanic temperatures, yielding an enrichment of +1.0 to +2.5 ‰ in the Nordic seas (Figure 3-a). Secondly, we can detect changes due to modified circulation following the freshwater influence, which induces a slight enrichment of +0.5‰ in the west Atlantic (Figure 3-b), and lastly changes due to injection of strongly depleted meltwater which causes a dilution of the $\delta^{18}O$ signature in the seawater (Figure 3-c). In this case, the entire region becomes increasingly depleted, with signature changes of -1.0‰ to -2.0‰. While this entanglement is demonstrated for the 0.2 Sv case, these effects are still present in the weaker injection scenarios. As noted earlier, the perturbation of 0.05 Sv yields a markedly smaller RMSE between the reconstructions and the simulation compared to the other injection experiments and might be a suitable representation of the climate dynamics at work at 130 ka BP. Yet, in order to attain these isotopic and temperature values in the simulation, the injection of freshwater needs to be sustained for at least 300 years. This perturbation strength and duration would already result in a sea level increase of 1.4 meters. The proxy reconstructions cover a time span of 131 to 129 ka BP, and maintaining the injection for the entire period would imply a sea level increase of 9.3 meters; which is at the upper limit of the reconstructed sea level changes for the entire LIG period spanning from 130 to 115 ka BP[31,32]. Furthermore, the dilution effect described above would be continuously active during these 2000 years, leading to increasingly depleted $\delta^{18}O$ seawater values as the freshwater forcing is maintained. Therefore, although the 0.05 Sv injection scenario provides a possible explanation and yields the smallest model/data mismatch based upon the RMSE values, we also explore an alternative mechanism to explain the ocean state reconstructed in the proxy data.

Considering The Ocean State: Glacial Conditions Following Termination II

A new hypothesis studied here for the first time is the influence of the ocean's initial state. This provides an alternative mechanism explaining the proxy reconstructions, which does not rely on freshwater injection. We postulate that the AMOC may still have been in a weak state at 130 ka due to large HE-11[16] meltwater injections occurring earlier during the preceding deglaciation (T-II), and the North Atlantic may thus have still been in a "glacial" state. Circulation characteristics were dominated by the orbital/GHG forcing only after this freshwater source had ceased. To test this hypothesis, we mimic a transition from glacial to interglacial by initializing our model from a cold ocean state, which is an idealized representation of T-II (this experiment runs for a total of 2000 years, see Methods for further details). The simulated North Atlantic exhibits lower surface temperatures compared to PI, depleted $\delta^{18}O$ values, and enriched $\delta^{18}O_c$ values, along with a weaker AMOC state. This scenario offers a unique characteristic, which is not possible with the typical snapshot experiments described earlier. The transition out of a glacial-type ocean circulation towards an interglacial lasts several hundred years and is accompanied by similar temperature changes seen in the freshwater perturbation experiments (Figure 4a). However, the changes in the AMOC (Figure 4b) occur without any freshwater influence, thus no additional sea level changes would accompany such a transition. Therefore, we propose that this transition out of a glacial oceanic state towards an interglacial state is a further possible explanation to understand the features captured by the proxy reconstructions, which may be recording the near-surface temperature and $\delta^{18}O_c$ fingerprints of an AMOC transition rather than a freshwater perturbation.

Implications And Conclusions

In summary, we have shown that the reconstructions at 130ka might be best reproduced by a simulated transition between a weak and a strong AMOC. In our simulations, the ocean circulation remains at a level which mirrors the proxy reconstructions for ~750 years of simulation time if we initialize our model from an idealized T-II/140 ka boundary state (Figure 4). While a freshwater injection of strongly depleted meltwater (Figure 3b) is also able to produce a model/data fit; we discard this scenario due to the fact that a relatively long, permanent freshwater injection would result in sea level rise which is higher than suggested by reconstructions, as explained above. Thus, a glacial ocean state should be considered for initialization in order to correctly represent the onset of the LIG.

Finally, although it is beyond the scope of this work to determine a new definition indicative of "full interglacial conditions", it is clear that such a definition must include some description of the AMOC state. When designing PMIP-style model intercomparison projects[18,27] for the LIG, the potential for a transient ocean circulation state should be considered, as such a climate state provides challenges in interpretation. Since simulations of the AMOC are very model-dependent[28], any deductions made regarding model skill should need to be appropriately contextualized.

Future work needs to examine communalities and differences between T-II and the last deglaciation leading into the Holocene/Anthropocene as well as the onset of other interglacials. While Termination I and the deglaciation out of the Last Glacial Maximum has been well studied[29–32], examining the transitions from older glacial periods into the following interglacials have lately gained further interest from the paleoclimate community. Gaining insight into these transitions into past warmer climates will be of key importance in understanding a potential future transition to a warmer climate of the Earth caused by human activities.

References

1. Capron, E. *et al.* Challenges and research priorities to understand interactions between climate, ice sheets and global mean sea level during past interglacials. *Quaternary Science Reviews* **219**, 308–311 (2019).
2. Fischer, H. *et al.* Palaeoclimate constraints on the impact of 2 °C anthropogenic warming and beyond. *Nature Geoscience* **11**, 474–485 (2018).
3. Dutton, A. & Lambeck, K. Ice volume and sea level during the last interglacial. *Science* **337**, 216–219 (2012).
4. Dutton, A., Webster, J. M., Zwartz, D., Lambeck, K. & Wohlfarth, B. Tropical tales of polar ice: evidence of Last Interglacial polar ice sheet retreat recorded by fossil reefs of the granitic Seychelles islands. *Quaternary Science Reviews* **107 IS-**, 182–196 (2015).
5. Pfeiffer, M. & Lohmann, G. Greenland Ice Sheet influence on Last Interglacial climate: global sensitivity studies performed with an atmosphere–ocean general circulation model. *Clim. Past* **12**, 1313–1338 (2016).
6. Sutter, J., Gierz, P., Grosfeld, K., Thoma, M. & Lohmann, G. Ocean temperature thresholds for Last Interglacial West Antarctic Ice Sheet collapse. *Geophysical Research Letters* **43**, 2675–2682 (2016).
7. DeConto, R. M. & Pollard, D. Contribution of Antarctica to past and future sea-level rise. *Nature* **531**, 591–597 (2016).
8. Govin, A. *et al.* Sequence of events from the onset to the demise of the Last Interglacial: Evaluating strengths and limitations of chronologies used in climatic archives. *Quaternary Science Reviews* **129**, 1–36 (2015).
9. Deaney, E. L., Barker, S. & van de Flierdt, T. Timing and nature of AMOC recovery across Termination 2 and magnitude of deglacial CO_2 change. *Nature Communications* **8**, 14595 (2017).
10. Turney, C. S. M. & Jones, R. T. Does the Agulhas Current amplify global temperatures during super-interglacials? *Journal of Quaternary Science* **25**, 839–843 (2010).

11. McKay, N. P., Overpeck, J. T. & Otto-Bliesner, B. L. The role of ocean thermal expansion in Last Interglacial sea level rise. *Geophysical Research Letters* **38** (2011).
12. Capron, E., Govin, A., Feng, R., Otto-Bliesner, B. L. & Wolff, E. W. Critical evaluation of climate syntheses to benchmark CMIP6/PMIP4 127 ka Last Interglacial simulations in the high-latitude regions. *Quaternary Science Reviews* **168**, 137–150 (2017).
13. Hoffman, J. S., Clark, P. U., Parnell, A. C. & He, F. Regional and global sea-surface temperatures during the last interglaciation. *Science* **355**, 276–279 (2017).
14. Stone, E. J. *et al.* Impact of melt water on high latitude early Last Interglacial climate. *Climate of the Past*, 1–22 (2016).
15. Govin, A. *et al.* Persistent influence of ice sheet melting on high northern latitude climate during the early Last Interglacial. *Clim. Past* **8**, 483–507 (2012).
16. Langebroek, P. M. & Nisancioglu, K. H. Simulating last interglacial climate with NorESM: role of insolation and greenhouse gases in the timing of peak warmth. *Climate of the Past* **10**, 1305–1318 (2014).
17. Past Interglacials Working Group of PAGES. Interglacials of the last 800,000 years. *Reviews of Geophysics* **54**, 162–219 (2016).
18. Menviel, L. *et al.* The penultimate deglaciation: protocol for PMIP4 transient numerical simulations between 140 and 127, version 1.0. *Geoscientific Model Development Discussions* 1–58 (2019) doi:https://doi.org/10.5194/gmd-2019-41.
19. EPICA community members. Eight glacial cycles from an Antarctic ice core. *Nature* **429**, 623–628 (2004).
20. Masson-Delmotte, V. *et al.* Information from Paleoclimate Archives. 82.
21. Gierz, P., Werner, M. & Lohmann, G. Simulating climate and stable water isotopes during the Last Interglacial using a coupled climate-isotope model. *Journal of Advances in Modeling Earth Systems* **9**, 2027–2045 (2017).
22. Lüthi, D. *et al.* High-resolution carbon dioxide concentration record 650,000-800,000[thinsp]years before present. *Nature* **453**, 379–382 (2008).
23. Loulergue, L. *et al.* Orbital and millennial-scale features of atmospheric CH4 over the past 800,000-years. *Nature* **453**, 383–386 (2008).
24. Spahni, R. *et al.* Atmospheric Methane and Nitrous Oxide of the Late Pleistocene from Antarctic Ice Cores. *Science* **310**, 1317–1321 (2005).
25. Berger, A. & Loutre, M. F. Insolation values for the climate of the last 10 million years. *Quaternary Science Reviews* **10**, 297–317 (1991).
26. Stocker, T. F. & Johnsen, S. J. A minimum thermodynamic model for the bipolar seesaw. *Paleoceanography* **18**, (2003).
27. Otto-Bliesner, B. L. *et al.* The PMIP4 contribution to CMIP6 – Part 2: Two interglacials, scientific objective and experimental design for Holocene and Last Interglacial simulations. *Geoscientific*

Model Development **10**, 3979–4003 (2017).

28. Kageyama, M. *et al.* Climatic impacts of fresh water hosing under Last Glacial Maximum conditions: a multi-model study. *Clim. Past* **9**, 935–953 (2013).
29. Eisenman, I., Bitz, C. M. & Tziperman, E. Rain driven by receding ice sheets as a cause of past climate change. *Paleoceanography* **24**, (2009).
30. Rossi, C., Bajo, P., Lozano, R. P. & Hellstrom, J. Younger Dryas to Early Holocene paleoclimate in Cantabria (N Spain): Constraints from speleothem Mg, annual fluorescence banding and stable isotope records. *Quaternary Science Reviews* **192**, 71–85 (2018).
31. Lohmann, G. & Schulz, M. Reconciling Bølling Warmth with peak deglacial meltwater discharge. *Paleoceanography* **15**, 537–540 (2000).
32. Weaver, A. J., Saenko, O. A., Clark, P. U. & Mitrovica, J. X. Meltwater pulse 1A from Antarctica as a trigger of the Bølling-Allerød warm interval. *Science* **299**, 1709–1713 (2003).

Figures

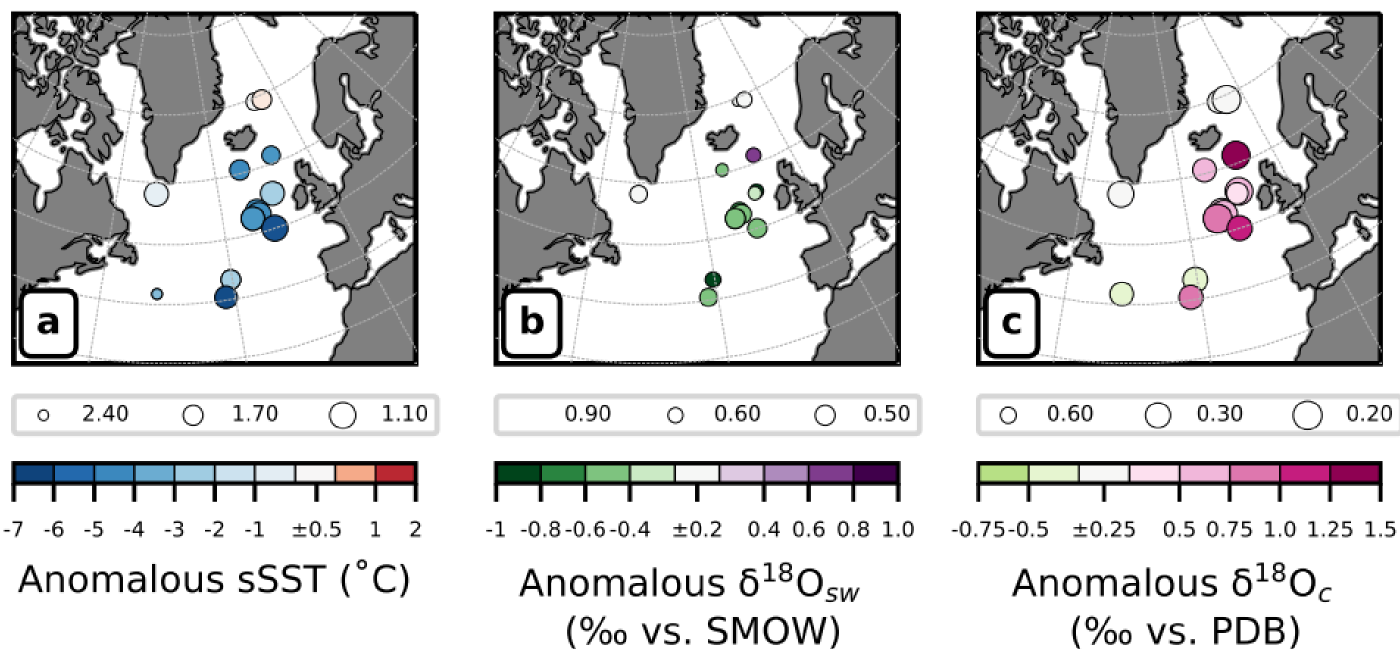

Figure 1

We use a temporally aligned synthesis of North Atlantic SSTs together with new reconstructions of the isotopic composition of seawater (δ18Osw) and planktic foraminiferal calcite (δ18Oc).

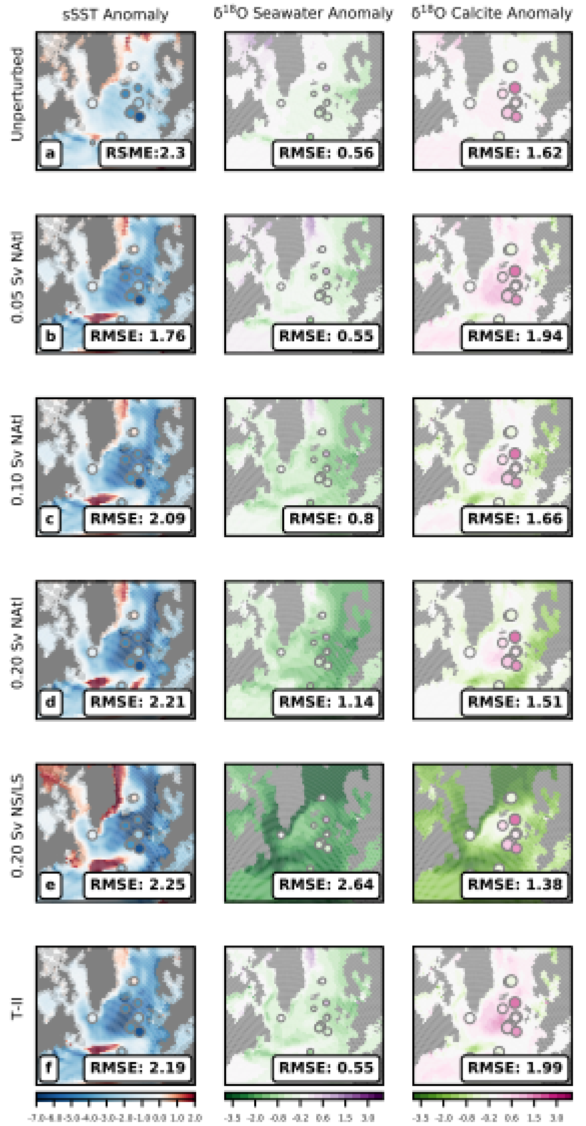

Figure 2

Increasing the freshwater perturbation results in i) a more pronounced North Atlantic cooling relative to the unperturbed state (Figure 2a-d, left panel), and ii) a tendency towards more depleted values in both δ18Osw and δ18Oc. (Figure 2a-d, middle and right panels).

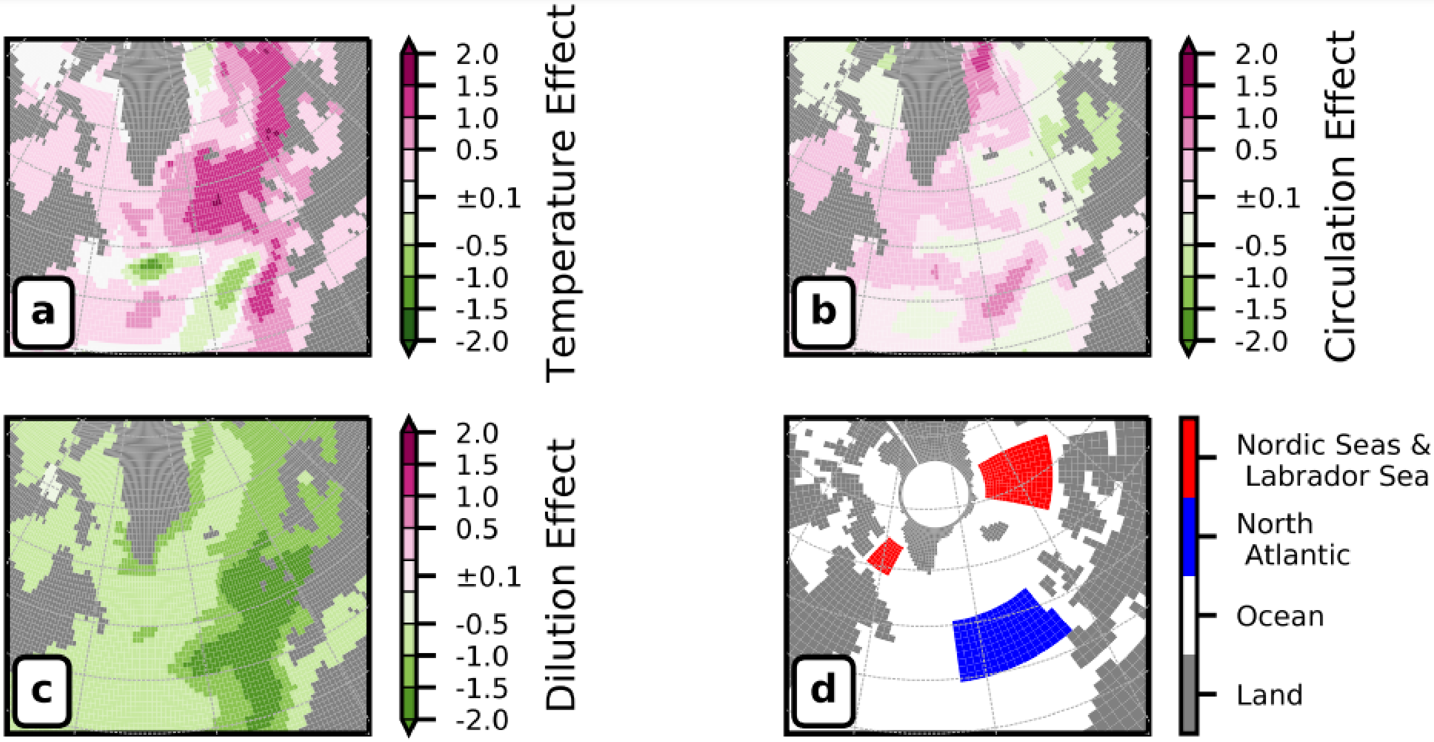

Figure 3

We are able to determine δ18Oc changes purely due to oceanic temperatures, yielding an enrichment of +1.0 to +2.5 ‰ in the Nordic seas (Figure 3-a). Secondly, we can detect changes due to modified circulation following the freshwater influence, which induces a slight enrichment of +0.5‰ in the west Atlantic (Figure 3-b), and lastly changes due to injection of strongly depleted meltwater which causes a dilution of the δ18O signature in the seawater (Figure 3-c).

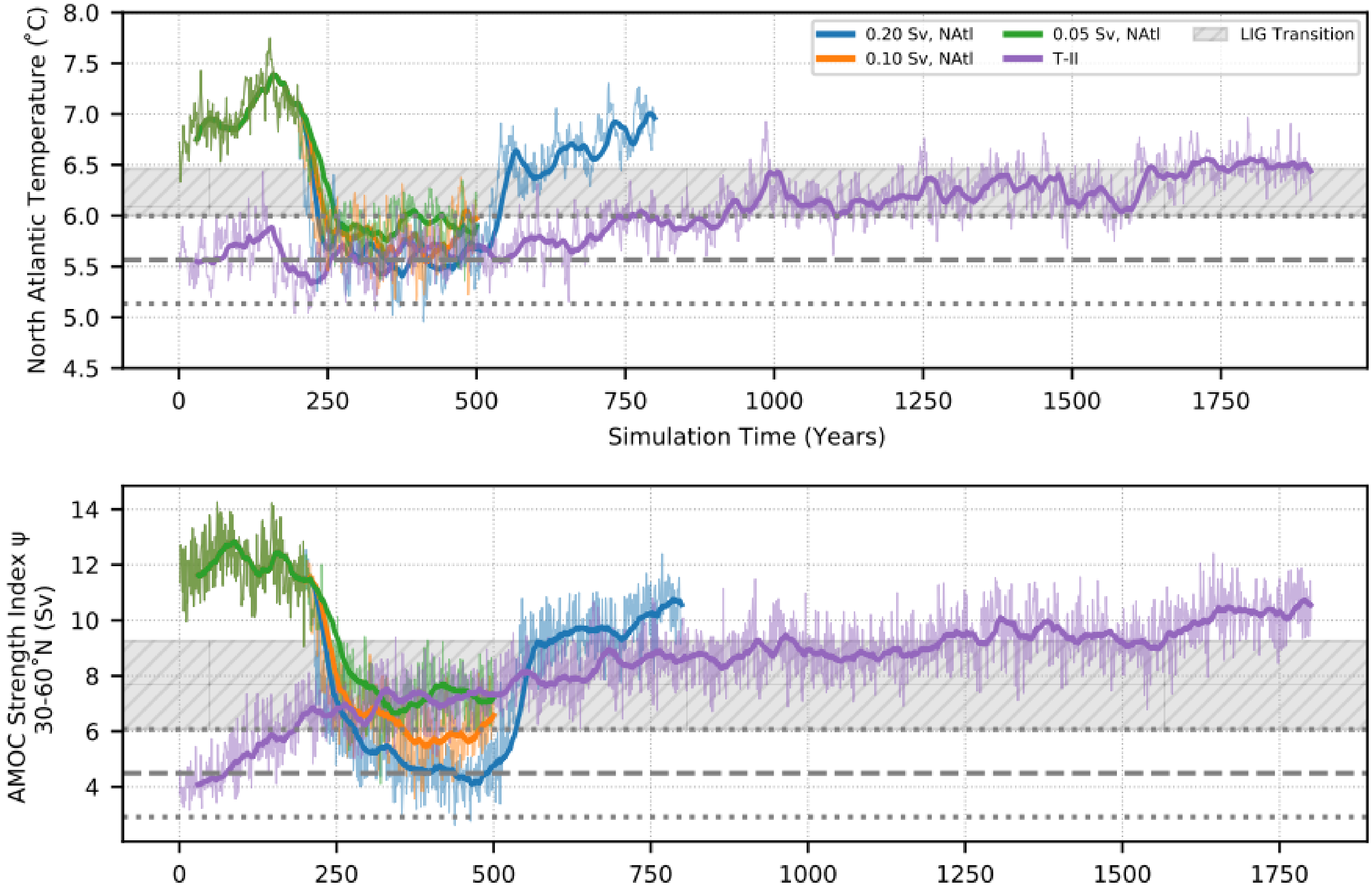

Figure 4

The ocean circulation remains at a level which mirrors the proxy reconstructions for ~750 years of simulation time if we initialize our model from an idealized T-II/140 ka boundary state.

Supplementary Files

This is a list of supplementary files associated with this preprint. Click to download.

- Table1.xlsx
- FigureS1.pdf
- FigureS2.pdf
- FigureS3.pdf
- FigureS4.pdf
- SUPPLEMENTTheOnsetoftheLastInterglacialandTransientAMOCFingerprints.docx